

## D-5-4

## A 2.4 GHz Differential Wavelet Generator in 0.18 $\mu\text{m}$ CMOS for 1.4 Gbps UWB Impulse Radio in Wireless Inter/Intra-Chip Data Communication

Pran Kanai Saha, Nobuo Sasaki and Takamaro Kikkawa

Research Center for Nanodevices and Systems, Hiroshima University  
1-4-2 Kagamiyama, Higashi Hiroshima 739-8527, JAPAN

Phone:+81-82-424-6265 Email:sahapk@sxsys.hiroshima-u.ac.jp, kikkawa@sxsys.hiroshima-u.ac.jp

### 1. Introduction

To meet the challenge of 3D-intergration in future ULSI, inter/intra-chip communication based on capacitive and inductive coupling technologies [1, 2] is limited in distance upto 300 $\mu\text{m}$  and the system has no multi-chip accessibility. To overcome these problems global wireless interconnection which utilizes electromagnetic wave transmission by using integrated antenna [3] and an ultra wideband (UWB) transceiver system has been proposed [4] as shown in Fig. 1. Among the different techniques for UWB system, impulse radio based UWB uses very short Gaussian monocycle pulses (GMP) as transmitted signal. Since the GMP transmission does not require any carrier, the transceiver circuit will be simple and occupies small area as it does not require any complex frequency recovery system. Generation of GMP wavelet using step recovery diode (SRD) based circuit for the present application is not acceptable because of SRD integration difficulties in CMOS technology [5]. In this work we present a new differential Gaussian monocycle pulse generator (DGMP) in 0.18 $\mu\text{m}$  CMOS which occupies small area and consumes low power. The transmission of the generated DGMP at a rate of 1.4 Gbps through integrated dipole antenna in the same Si-substrate is also verified by simulation and results are presented here.

### 2. Gaussian Monocycle Pulse Generation

A differentiator generates two impulses at the rising and falling edges of the input if the input of the differentiator is a rectangular pulse as shown in Fig 2. The interval between the two impulses depends on the rectangular pulse duration ( $t_d$ ). If the duration is reduced, the negative impulse shifts to the left until it coincides with the end of the positive impulse and this forms Gaussian monocycle pulse as shown in Fig. 2(d). The GMP's duration ( $t_m$ ) depends on the rising ( $t_r$ ) and falling ( $t_f$ ) time of the zero interval rectangular pulse (i.e. Triangular pulse (TP) which has Gaussian properties) and is given as  $t_m=t_r+t_f$ . The GMP center frequency ( $f_c$ ) will be reciprocal of  $t_m$ . In this work the above mentioned technique has been implemented in a CMOS circuit to generate the differential GMP wavelet for impulse based UWB transceiver.

### 3. GMP Circuit and Simulation

A schematic block diagram of the developed differential GMP circuit is shown in Fig. 3. The circuit is implemented in 0.18  $\mu\text{m}$  CMOS process. Each circuit block of the schematic and its layout is shown in Fig. 4. Simulation is done with extracted netlist by HSPICE. Parasitic resistance, capacitance and coupling capacitance are also taken into account during simulation.

The differential voltage controlled ring oscillator (VCO) first generates rectangular shaped pulse with a frequency of 1.408 GHz as shown in Fig. 5(a). The triangular pulse (TP) is then generated from the VCO output by using digital pulse shaping circuit which consists of a voltage controlled non-inverting buffer delay circuit, Exclusive-or (XOR) gate and AND gate (shown in Fig. 4(b)). The delay circuit shifts the rectangular shaped pulse by a time which is slightly less than the rising time (0.185ns) of the VCO output. The triangular pulse with a rising time of 0.12 ns and falling time of 0.239 ns is generated as shown in Fig. 5(b) from VCO output

and its delayed output. The Fig. 5(c) shows that FFT of this triangular pulse is similar to that of Gaussian pulse. The triangular pulse is then differentiated to generate GMP. The differentiator (shown in Fig. 4(c)) is designed using metal-insulator-metal (MIM) capacitor (C) and poly resistor (R) in such a way that it behaves as close as to ideal differentiator in the frequency range of interest. The generated GMP from simulation is shown in Fig. 6(a). The amplitude of the GMP depends on derivative time constant (RC),  $t_r$  and  $t_f$ . The amplitude of the negative impulse of GMP is found to be the half of that of positive impulse because  $t_f$  is twice of the  $t_r$ . The GMP duration is found to be 0.41 ns which is slightly higher than that of  $t_r+t_f$ . To reduce the common mode noise and transmit the GMP by integrated dipole antenna, single ended GMP is converted to differential GMP by using single input differential output (SIDO) amplifier as shown in Fig. 4(c). The generated differential Gaussian monocycle (DGMP) is shown in Fig. 6 (b). The DGMP is further amplified by differential output amplifier (shown in Fig. 4(c)). The Output amplifier has a voltage gain of 7.28 dB at the center frequency of GMP (2.4 GHz) and wide bandwidth. The amplified DGMP is shown in Fig. 6(c). The FFT of GMP as shown in Fig. 6(d) depicts that the GMP has a center frequency ( $f_c$ ) of 2.4 GHz and 3-dB bandwidth (BW) of 2.8 GHz. However further increasing of  $f_c$  is possible by generating the short rising and falling edge of TP. A source follower circuit (shown in Fig. 3) is used to avoid reflection due to impedance mismatch between the DGMP circuit and transmitting antenna.

### 4. Simulation of GMP Transmission/Reception

Characteristics (S-parameter) of 6 mm long transmitting and receiving dipole antenna pair on a silicon substrate (shown in Fig.1) was evaluated by MW Studio and was then verified by measurement [6]. This verified S-parameters are used to generate the HSPICE netlist macromodel by using EMtoSPICE<sup>TM</sup> converter [7]. The accuracy of generated macromodel is verified by comparing the S-parameter obtained from HSPICE simulation with that from the MW studio as shown in Fig. 7. To confirm the transmission and reception of GMP by integrated antenna in silicon, simulation is done together with the DGMP layout extracted netlist and HSPICE netlist macromodel of integrated antenna pair. The simulation results for different communication distance (d, 1mm-5mm) are shown in Fig. 8. The Fig. 8 shows that the received signal is the derivative of the transmitted signal due to antenna effect and the transmission and reception is achieved at the rate of 1.4 GHz.

### 5. Conclusion

The architecture of 2.4 GHz DGMP generation for UWB impulse based radio system in wireless inter/intra-chip data communication is discussed. The developed DGMP generation circuit occupies a small area (0.06  $\text{mm}^2$ ) and consumes a total power of 44 mW in transmit mode from 1.8 V supply. Transmission and reception of DGMP by 6 mm long integrated dipole antenna pair in silicon is confirmed by simulation. The simulation shows that a DGMP repetition rate is 1.4 GHz thus a data transmission rate of 1.4Gbps could be achieved.

### Acknowledgements

This work is supported by the Ministry of Education, Culture, Sports, Science and Technology, Japan under 21<sup>st</sup> Century COE program, Hiroshima University.

### References

[1] K. Kanda et al, ISSCC Digest Tech. Papers p. 186 Feb. 2003.  
 [2] D. Mizoguchi et al. ISSCC Digest Tech. Papers p. 142 Feb. 2004.  
 [3] A. B. M. H. Rashid, et al. IEEE EDL, vol. 23, No. 12, Dec 2002, p. 731  
 [4] P.K. Saha et al. Proc. ISSSTA 2004, Australia, p. 962.  
 [5] Jeongwoo et al. , IEEE microwave, wireless and components Lett., vol. 12, No. 6, June 2002, p. 206.  
 [6] S. Watanabe et al. Proc. IEEE AP-S Symposium, USA, 2004, p. 2277.  
 [7] EMtoSPICE converter, EM Wonder ,USA.

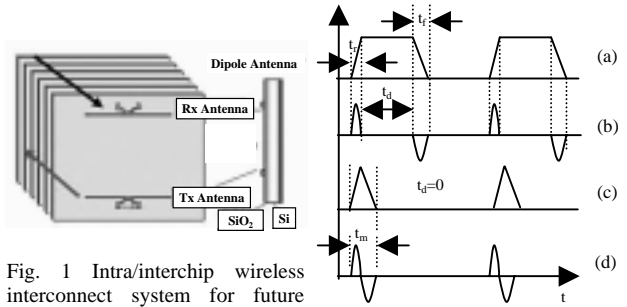


Fig. 1 Intra/interchip wireless interconnect system for future ULSI.

Fig. 2 Generation of Gaussian monocycle pulse. (a) Rectangular pulse. (b) Gaussian Impulse. (c) Triangular pulse. (d) Gaussian monocycle pulse.

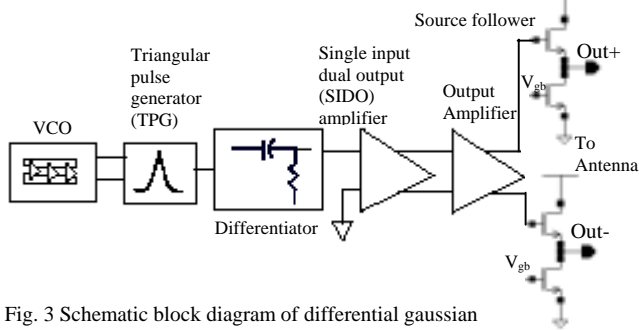


Fig. 3 Schematic block diagram of differential gaussian monocycle pulse (DGMP) wavelet generator.

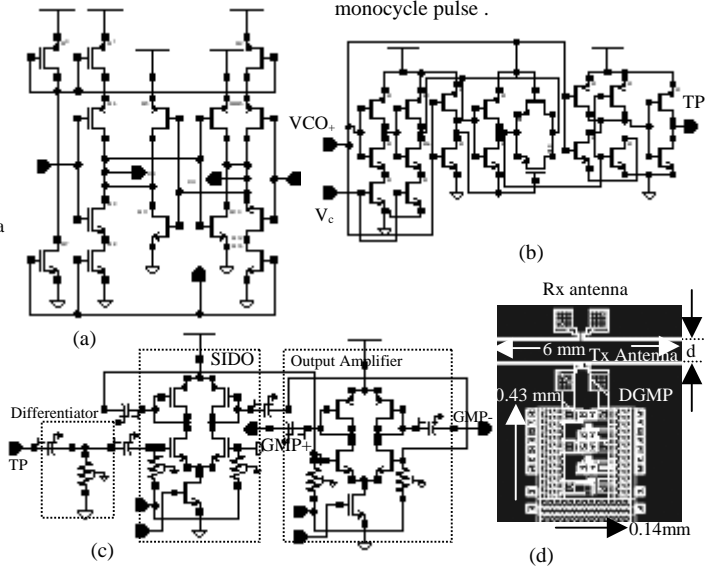


Fig. 4 Circuit block of DGMP. (a) Differential delay cell for VCO. (b) TP generation circuit. (c) DGMP generation circuit. (d) Circuit layout. Antenna size is not in scale.

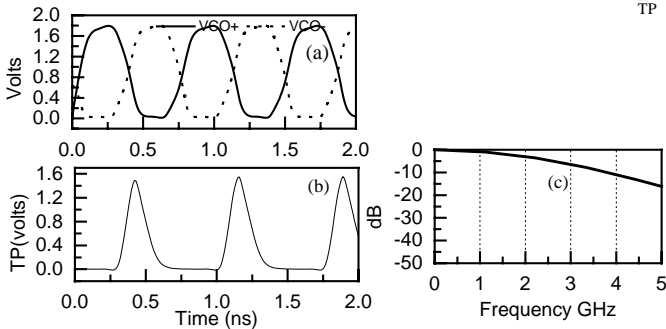


Fig. 5 Generation of triangular pulse from VCO output. (a) VCO output. (b) Triangular Pulse (TP). (c) FFT of TP.

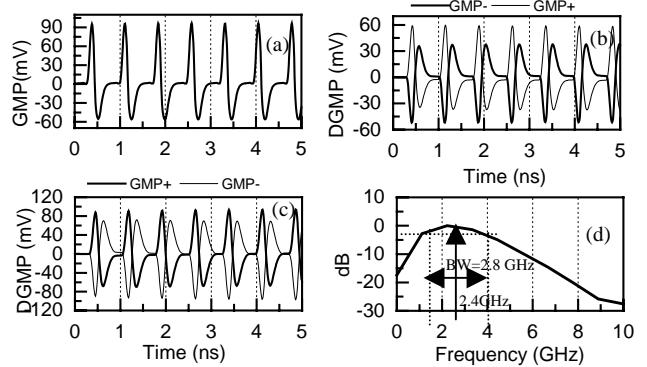


Fig. 6 Generation of GMP from TP. (a) Single ended GMP. (b) DGMP after SIDO circuit (c) DGMP after output amplifier. (d) FFT of GMP.

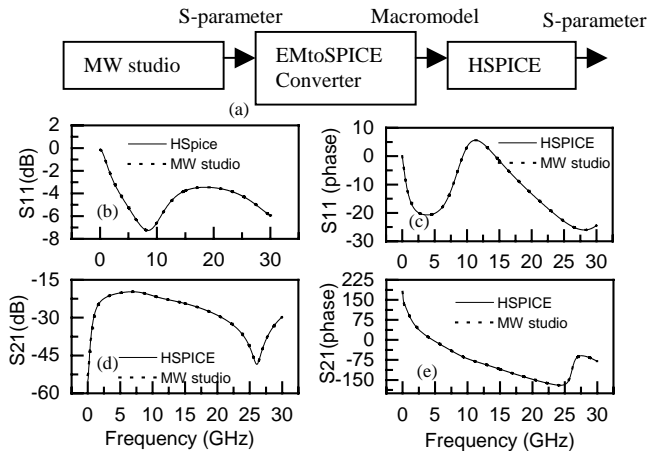


Fig. 7 Comparison of S-parameter for  $d=1\text{mm}$ . (a) Generation of HSPICE netlist macromodel for Tx-Rx antenna pair from S-parameter. (b) Magnitude of reflection co-efficient ( $S_{11}$ ). (c) Phase of  $S_{11}$ . (d) Magnitude of transmission co-efficient ( $S_{21}$ ). (e) Phase of  $S_{21}$ .

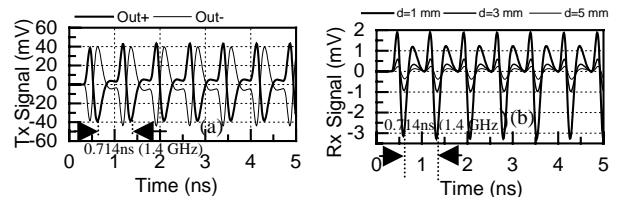


Fig. 8 GMP transmission using integrated antenna in silicon. (a) Transmitted signal. (b) Received signal when receiving antenna was terminated by 100 Ohms load for different communication distance.